

**FINITE ELEMENT ANALYSIS OF LORD-SHULMAN
THERMOELASTICITY TIME-DEPENDENT PROBLEM****V. Stelmashchuk, R. Petryshyn, H. Shynkarenko***Ivan Franko National University of Lviv,
1, Universytetska str., 79000, Lviv, Ukraine**e-mail: vitalii.stelmashchuk@lnu.edu.ua,**roman.petryshyn.apmi@lnu.edu.ua, heorhiy.shynkarenko@lnu.edu.ua*

The initial boundary value problem for Lord-Shulman thermoelasticity is considered. It is then transformed into the corresponding variational one. Using Galerkin semidiscretization by spatial variables with finite element basis functions the variational problem is reduced to matrix Cauchy problem. For time discretization of the Cauchy problem we adopt a hybrid time integration scheme (based on Newmark scheme and generalized trapezoidal rule) that was initially developed for Lord-Shulman thermopiezoelectricity problem. In numerical experiments we consider a ramp-type heating of the edge of a solid bar. The solutions obtained by the proposed numerical scheme are then compared with the ones for the corresponding Lord-Shulman thermopiezoelectricity problem which are available in the literature. In particular, it is shown that piezoeffect and pyroeffect make a noticeable influence of the behaviour of the stress wave in the solid bar. Besides, the numerical results are in accordance with the ones obtained by other researchers via other solution techniques.

Key words: Lord-Shulman thermoelasticity, initial boundary value problem, variational problem, finite element method, Newmark scheme, generalized trapezoidal rule.

1. INTRODUCTION

The classical theory of coupled thermoelasticity assumes the infinite speed of thermal waves propagation. Lord and Shulman [11] proposed to overcome this drawback by introducing a “relaxation time parameter” t_0 . Although the work of Lord and Shulman was done decades ago, the model still draws researchers’ attention nowadays, see, for example, [2–4, 9, 10, 16, 17]. Apart from thermoelasticity, the Lord-Shulman model is also frequently used for coupled thermopiezoelectricity problems [6–8, 12, 15]. Some of the authors of this work also published their previous papers on the topic of Lord-Shulman thermopiezoelectricity, see [12–14].

In paper [13] the well-posedness of coupled Lord-Shulman thermopiezoelectricity problem is proved which also suggests the conditions of well-posedness of the corresponding thermoelasticity problem as its partial case. In [12] and [14] two slightly different numerical schemes are proposed for numerical solution of this thermopiezoelectricity problem. In this paper we adopt the solution technique from the work [14] for solution of Lord-Shulman thermoelasticity initial boundary value problem and compare the obtained numerical results with the ones depicted in [14] and [15].

In section 2 the initial boundary value problem of Lord-Shulman thermoelasticity is formulated. In section 3 it is transformed into the corresponding variational problem. Section 4 describes Galerkin semi-discretization of the variational problem with finite element basis functions. Section 5 is devoted to the adoption of hybrid time integration scheme from [14] for solution of the obtained semi-discrete matrix Cauchy problem. Section 6 describes the results of the numerical experiments. Finally, in section 7 the conclusions are made.

2. INITIAL BOUNDARY VALUE PROBLEM

The initial boundary value problem of Lord-Shulman thermoelasticity is a partial case of the corresponding thermopiezoelectricity problem that is depicted in some of the authors' previous works [12–14].

We consider a bounded connected domain Ω of points $\mathbf{x} = (x_1, \dots, x_d) \in \mathbb{R}^d$ with Lipschitz-continuous boundary $\partial\Omega = \Gamma$. The thermoelastic behavior of a solid occupying the domain Ω is under our interest during the time interval $[0, T]$, $0 < T < +\infty$.

The goal is to find a vector of elastic displacements $\mathbf{u} = \{u_i(\mathbf{x}, t)\}_{i=1}^d$, temperature increment $\theta = \theta(\mathbf{x}, t)$ and a vector of heat fluxes $\mathbf{q} = \{q_i(\mathbf{x}, t)\}_{i=1}^d$ which satisfy the following system of partial differential equations in $\Omega \times (0, T]$ (here and everywhere below the ordinary summation by repetitive indices is expected):

$$\rho(u_i'' - f_i) - \sigma_{ij,j} = 0, \quad (1)$$

$$\rho(T_0 S' - w) + q_{i,i} = 0, \quad (2)$$

$$t_0 q_i' + q_i = -\lambda_{ij} \theta_{,j}. \quad (3)$$

Here and everywhere below a prime symbol ' means partial differentiation by a time variable and a partial derivative by a corresponding component of the spatial variable is indicated by a comma in the subscript, i.e. $g_{,k} = \partial g / \partial x_k$. The above expressions (1)–(3) are equation of motion, heat conduction equation and a modified Fourier's law correspondingly.

The parameter t_0 is called “relaxation time” and distinguishes the Lord-Shulman thermoelasticity model [11] from the classical one and resolves the problem of infinite speed of heat propagation. After introducing the artificial coefficients κ_{ij} such that $T_0 \kappa_{ij} \lambda_{jm} = \delta_{im}$, where δ_{im} is a unit tensor, the modified Fourier's law (3) can be rewritten in a more convenient form that is used in works [12–14] :

$$t_0 \kappa_{ij} q_i' + \kappa_{ij} q_i = -T_0^{-1} \theta_{,j}. \quad (4)$$

The stress tensor σ_{ij} used in equation of motion (1) is determined by the constitutive equation below:

$$\sigma_{ij} = c_{ijkl} \varepsilon_{km} - \beta_{ij} \theta + a_{ijkl} \varepsilon'_{km}. \quad (5)$$

The entropy density S used in heat conduction equation (2) is defined by:

$$\rho S = \rho c_v T_0^{-1} \theta + \beta_{ij} \varepsilon_{ij}. \quad (6)$$

The strain tensor $\varepsilon = \{\varepsilon_{km}\}_{k,m=1}^d$ used in (5) and (6) is:

$$\varepsilon_{km} = \varepsilon_{km}(u) = \frac{1}{2}(u_{k,m} + u_{m,k}). \quad (7)$$

The mass density of a solid is ρ , c_v is a specific heat coefficient. T_0 is a fixed uniform reference temperature. Vector f_i defines mechanical volume forces and w determines volume heat forces. Tensors $\{a_{ijkl}\}$ and $\{c_{ijkl}\}$ are the viscosity and elasticity coefficients of a solid and satisfy common conditions of symmetry and ellipticity.

Notations λ_{ij} , $\beta_{ij} = c_{ijkl} \alpha_{km}$, α_{km} define the symmetrical and elliptical heat conductivity, stress-temperature and thermal expansion coefficients respectively.

The system of partial differential equations defined by expressions (1), (2) and (4) is complemented by the corresponding boundary and initial conditions.

The boundary conditions are [12–14]:

$$\begin{cases} u_i = 0 & \text{on } \Gamma_u \times [0, T], \Gamma_u \subset \Gamma, \text{mes}(\Gamma_u) > 0, \\ \sigma_{ij}n_j = \bar{\sigma}_i & \text{on } \Gamma_\sigma \times [0, T], \Gamma_\sigma := \Gamma \setminus \Gamma_u, \\ \theta = 0 & \text{on } \Gamma_\theta \times [0, T], \Gamma_\theta \subset \Gamma, \text{mes}(\Gamma_\theta) > 0, \\ q_i n_i = 0 & \text{on } \Gamma_q \times [0, T], \Gamma_q := \Gamma \setminus \Gamma_\theta, \end{cases} \quad (8)$$

where $\mathbf{n} = (n_1, \dots, n_d)$ is a unit outer normal vector.

The initial conditions are [12–14]:

$$\mathbf{u}|_{t=0} = \mathbf{u}_0, \quad \mathbf{u}'|_{t=0} = \mathbf{v}_0, \quad \theta|_{t=0} = \theta_0, \quad \mathbf{q}|_{t=0} = \mathbf{q}_0 \quad \text{in } \Omega. \quad (9)$$

3. VARIATIONAL PROBLEM AND ITS WELL-POSEDNESS

Let us introduce the following spaces of admissible unknown functions [12–14]:

$$\begin{aligned} \mathbf{V} &= \left\{ \mathbf{v} \in [H^1(\Omega)]^d : \mathbf{v} = 0 \text{ on } \Gamma_u \right\}, \\ Z &= \left\{ \zeta \in H^1(\Omega) : \zeta = 0 \text{ on } \Gamma_\theta \right\}, \\ \mathbf{H} &= \left\{ \mathbf{y} \in H(\text{div}; \Omega) : y_i, \text{div } \mathbf{y} \in L^2(\Omega), y_i n_i = 0 \text{ on } \Gamma_q \right\}. \end{aligned} \quad (10)$$

Here $H^m(\Omega)$ is a standard Sobolev space.

Also we denote $\Phi := \mathbf{V} \times Z \times \mathbf{H}$. As a result we get the following variational problem statement for the original Lord-Shulman thermoelasticity initial boundary value problem defined by equations (1), (2), (4), boundary conditions (8) and initial conditions (9):

$$\begin{cases} \text{find } \psi = (\mathbf{u}, \theta, \mathbf{q}) \in L^2(0, T; \Phi) \text{ such that} \\ m(\mathbf{u}''(t), \mathbf{v}) + a(\mathbf{u}'(t), \mathbf{v}) + c(\mathbf{u}(t), \mathbf{v}) - \beta(\theta(t), \mathbf{v}) = \langle \mathbf{l}_\sigma(t), \mathbf{v} \rangle, \\ s(\theta'(t), \zeta) + T_0^{-1}(\text{div } \mathbf{q}(t), \zeta) + \beta(\zeta, \mathbf{u}'(t)) = \langle l_\theta(t), \zeta \rangle, \\ t_0 \kappa(\mathbf{q}'(t), \mathbf{y}) - T_0^{-1}(\text{div } \mathbf{y}, \theta(t)) + \kappa(\mathbf{q}(t), \mathbf{y}) = 0 \quad \forall t \in (0, T], \\ m(\mathbf{u}'(0) - \mathbf{v}_0, \mathbf{v}) = 0, \quad c(\mathbf{u}(0) - \mathbf{u}_0, \mathbf{v}) = 0, \\ s(\theta(0) - \theta_0, \zeta) = 0, \\ \kappa(\mathbf{q}(0) - \mathbf{q}_0, \mathbf{y}) = 0 \quad \forall \varphi = (\mathbf{v}, \zeta, \mathbf{y}) \in \Phi, \end{cases} \quad (11)$$

where the bilinear and linear forms used above are defined as follows:

$$\begin{aligned} m(\mathbf{u}, \mathbf{v}) &= \int_{\Omega} \rho u_i v_i dx, \quad a(\mathbf{u}, \mathbf{v}) = \int_{\Omega} a_{ijkl} \varepsilon_{ij}(\mathbf{u}) \varepsilon_{kl}(\mathbf{v}) dx, \\ c(\mathbf{u}, \mathbf{v}) &= \int_{\Omega} c_{ijkl} \varepsilon_{ij}(\mathbf{u}) \varepsilon_{kl}(\mathbf{v}) dx, \quad \beta(\zeta, \mathbf{v}) = \int_{\Omega} \beta_{ij} \varepsilon_{ij}(\mathbf{v}) \zeta dx, \\ s(\theta, \zeta) &= \int_{\Omega} \rho c_v T_0^{-1} \theta \zeta dx, \quad \kappa(\mathbf{q}, \mathbf{y}) = \int_{\Omega} \kappa_{lm} q_l y_m dx, \\ \langle \mathbf{l}_\sigma, \mathbf{v} \rangle &= \int_{\Omega} \rho f_i v_i dx + \int_{\Gamma_\sigma} \bar{\sigma}_i v_i d\gamma, \quad \langle l_\theta, \zeta \rangle = \int_{\Omega} T_0^{-1} \rho w \zeta dx \\ \forall \mathbf{u}, \mathbf{v} \in \mathbf{V}, \forall \theta, \zeta \in Z, \forall \mathbf{q}, \mathbf{y} \in \mathbf{H}. \end{aligned} \quad (12)$$

Here we also use a symbol $\text{div } \mathbf{y} := y_{i,i}$ for each vector function $\mathbf{y} \in [H^1(\Omega)]^d$. Notation $(z, w) = \int_{\Omega} z w dx$ defines a scalar product $\forall z, w \in L^2(\Omega)$.

As it is done in [12, 13], we can now introduce energy norms based on bilinear forms defined in (12), i.e. $\|\mathbf{u}'(t)\|_m^2 = m(\mathbf{u}, \mathbf{u})$, etc. Also, similar to [12, 13] we define the notations for energy norms that determine a kinetic energy of a solid:

$$|\psi(t)|_{\Phi}^2 := \frac{1}{2} [\|\mathbf{u}'(t)\|_m^2 + t_0 \|\mathbf{q}(t)\|_{\kappa}^2], \quad (13)$$

its potential energy:

$$\|\psi(t)\|_{\Phi}^2 := \frac{1}{2} [\|\mathbf{u}(t)\|_c^2 + \|\theta(t)\|_s^2], \quad (14)$$

and energy dissipation:

$$|||\psi(t)|||_{\Phi}^2 := \|\mathbf{u}'(t)\|_a^2 + \|\mathbf{q}(t)\|_{\kappa}^2. \quad (15)$$

Besides, we introduce the notation for the sum of linear forms similar to the one used in [12–14]:

$$\langle N(t), \varphi \rangle := \langle \mathbf{l}_{\sigma}(t), \mathbf{v} \rangle + \langle l_{\theta}(t), \zeta \rangle, \quad \forall \varphi = (\mathbf{v}, \zeta, \mathbf{y}) \in \Phi. \quad (16)$$

Then the solution $\psi = (\mathbf{u}, \theta, \mathbf{q})$ of the variational problem of Lord-Shulman thermoelasticity (11) satisfies the following **energy balance law** similar to the one for Lord-Shulman thermopiezoelectricity problem described in [12–14]:

$$\begin{aligned} |\psi(t)|_{\Phi}^2 + \|\psi(t)\|_{\Phi}^2 + \int_0^t |||\psi(s)|||_{\Phi}^2 ds = \\ = |\psi(0)|_{\Phi}^2 + \|\psi(0)\|_{\Phi}^2 + \int_0^t \langle N(s), \psi \rangle ds \quad \forall t \in [0, T]. \end{aligned} \quad (17)$$

The potential energy (14) and energy dissipation (15) for our thermoelasticity problem differ from the corresponding ones for thermopiezoelectricity problem only by some positive terms and the definition of the kinetic energy (13) is completely identical to the one for thermopiezoelectricity problem. Since the proof of well-posedness of Lord-Shulman thermopiezoelectricity variational problem is done in [13] based on energy balance law, we can conclude that all the steps of this proof procedure remain valid for the variational problem (11). Thus, the Lord-Shulman thermoelasticity variational problem (11) is well-posed as a partial case of the corresponding thermopiezoelectricity problem.

4. FINITE ELEMENT SEMI-DISCRETIZATION

Let us define in the space $\Phi := \mathbf{V} \times Z \times \mathbf{H}$ a sequence of finite-dimensional subspaces $\Phi_h := \mathbf{V}_h \times Z_h \times \mathbf{H}_h$, such that $\dim \Phi_h \rightarrow \infty$ when $h \rightarrow 0$ with the following density properties:

$$\left\{ \begin{array}{l} \forall \phi \in \Phi \cap [H^{k+1}(\Omega)]^{d+2}, \quad k \geq 1, \\ \exists \phi_h \in \Phi_h \quad \text{and} \quad C = \text{const} > 0 \text{ such that} \\ \|\phi - \phi_h\|_{m, \Omega} \leq Ch^{k+1-m} \|\phi\|_{k+1, \Omega}, \quad 0 \leq m \leq k. \end{array} \right. \quad (18)$$

Here k is the greatest degree of the polynomial that approximates the unknown solution (determined by the base functions of Φ_h). The norm $\|\cdot\|_{m, \Omega}$ is a norm in a standard Sobolev space $H^m(\Omega)$. Also, here and everywhere below the symbol C defines different positive constants that do not depend on the solutions of our problem.

For each fixed $h > 0$ a solution $\psi_h = (\mathbf{u}_h, \theta_h, \mathbf{q}_h)$ of the problem

$$\left\{ \begin{array}{l} \text{given } \psi_0 = (\mathbf{u}_0, \theta_0, \mathbf{q}_0), \mathbf{v}_0 \in \mathbf{V}_h \text{ and } (\mathbf{l}_\sigma, l_\vartheta, 0) \in L^2(0, T; \Phi'_h); \\ \text{find } \psi_h = (\mathbf{u}_h, \theta_h, \mathbf{q}_h) \in L^2(0, T; \Phi_h) \text{ such that} \\ m(\mathbf{u}_h''(t), \mathbf{v}) + a(\mathbf{u}_h'(t), \mathbf{v}) + c(\mathbf{u}_h(t), \mathbf{v}) - \beta(\theta_h(t), \mathbf{v}) = \langle \mathbf{l}_\sigma(t), \mathbf{v} \rangle, \\ s(\theta_h'(t), \zeta) + T_0^{-1}(\text{div} \mathbf{q}_h(t), \zeta) + \beta(\zeta, \mathbf{u}_h'(t)) = \langle l_\vartheta(t), \zeta \rangle, \\ t_0 \kappa(\mathbf{q}_h'(t), \mathbf{y}) - T_0^{-1}(\text{div} \mathbf{y}, \theta_h(t)) + \kappa(\mathbf{q}_h(t), \mathbf{y}) = 0 \quad \forall t \in (0, T], \\ m(\mathbf{u}_h'(0) - \mathbf{v}_0, \mathbf{v}) = 0, \quad c(\mathbf{u}_h(0) - \mathbf{u}_0, \mathbf{v}) = 0, \\ s(\theta_h(0) - \theta_0, \zeta) = 0, \\ \kappa(\mathbf{q}_h(0) - \mathbf{q}_0, \mathbf{y}) = 0 \quad \forall \varphi = (\mathbf{v}, \zeta, \mathbf{y}) \in \Phi_h, \end{array} \right. \quad (19)$$

is a semi-discrete Galerkin approximation of the solution $\psi = (\mathbf{u}, \theta, \mathbf{q})$ of the variational problem (11). The constant h is a space discretization parameter of the problem (11).

Let us fix some bases $\{\mathbf{v}_i\}$, $\{\zeta_i\}$, $\{\mathbf{y}_i\}$, in the approximation subspaces \mathbf{V}_h , Z_h and \mathbf{H}_h correspondingly. Those bases are selected by means of finite element method. Then our unknown solution functions can be represented as following expansions:

$$\begin{aligned} \mathbf{u}_h(x, t) &= \sum_{i=1}^{\dim \mathbf{V}_h} \mathbf{U}_i(t) \mathbf{v}_i(x), \\ \theta_h(x, t) &= \sum_{i=1}^{\dim Z_h} \Theta_i(t) \zeta_i(x), \\ \mathbf{q}_h(x, t) &= \sum_{i=1}^{\dim \mathbf{H}_h} \mathbf{Q}_i(t) \mathbf{y}_i(x). \end{aligned} \quad (20)$$

Substituting (20) into (19) we obtain a Cauchy problem for determining the unknown coefficients $\mathbf{U}(t) = \{\mathbf{U}_i(t)\}$, $\Theta(t) = \{\Theta_i(t)\}$ and $\mathbf{Q}(t) = \{\mathbf{Q}_i(t)\}$ of approximations \mathbf{u}_h , θ_h and \mathbf{q}_h :

$$\left\{ \begin{array}{l} \mathbf{M}\mathbf{U}''(t) + \mathbf{A}\mathbf{U}'(t) + \mathbf{C}\mathbf{U}(t) - \mathbf{B}^T \Theta(t) = \mathbf{L}_\sigma(t), \\ \mathbf{S}\Theta'(t) + \mathbf{W}^T \mathbf{Q}(t) + \mathbf{B}\mathbf{U}'(t) = \mathbf{L}_\vartheta(t), \\ \mathbf{K}[\mathbf{Q}(t) + t_0 \mathbf{Q}'(t)] - \mathbf{W}\Theta(t) = 0 \quad \forall t \in (0, T], \\ \mathbf{M}\mathbf{U}'(0) = \mathbf{V}^0, \quad \mathbf{C}\mathbf{U}(0) = \mathbf{U}^0, \\ \mathbf{S}\Theta(0) = \Theta^0, \quad \mathbf{K}\mathbf{Q}(0) = \mathbf{Q}^0, \end{array} \right. \quad (21)$$

The matrices and vectors used in (21) are calculated using the corresponding bilinear and linear forms defined in (12) by applying them to the base functions of the finite-dimensional subspaces \mathbf{V}_h , Z_h and \mathbf{H}_h , for example, $\mathbf{M} = \{m_{ij}\} = m(\mathbf{v}_i, \mathbf{v}_j)$, $\mathbf{S} = \{s_{ij}\} = s(\zeta_i, \zeta_j)$, etc. In general, a matrix denoted by a capital letter is formed by a bilinear form denoted by a respective lowercase letter. The vectors $\mathbf{L}_\sigma(t)$ and $\mathbf{L}_\vartheta(t)$ are formed using the corresponding linear forms:

$$\mathbf{L}_\sigma(t) = \{\langle l_\sigma(t), \mathbf{v}_i \rangle\}, \quad \mathbf{L}_\vartheta(t) = \{\langle l_\vartheta(t), \zeta_i \rangle\} \quad (22)$$

and vectors that represent the initial conditions are calculated via expressions:

$$\begin{aligned} \mathbf{V}^0 &= \{m(\mathbf{v}_0, \mathbf{v}_i)\}, \quad \mathbf{U}^0 = \{c(\mathbf{u}_0, \mathbf{v}_i)\}, \\ \Theta^0 &= \{s(\theta_0, \zeta_i)\}, \quad \mathbf{Q}^0 = \{\kappa(\mathbf{q}_0, \mathbf{y}_i)\}. \end{aligned} \quad (23)$$

Since matrices \mathbf{M} , \mathbf{S} and \mathbf{K} are positively defined, we can be sure that there exists a solution of the Cauchy problem (21).

5. TIME INTEGRATION SCHEME

For time discretization of the Cauchy problem (21) we consider a uniform partition of the time interval $[0, T]$ by nodes $t_j = j\Delta t$, $j = 0, 1, \dots, N_T$, where N_T is some fixed number and $T = N_T\Delta t$. Then we use a hybrid time integration scheme approach from [14].

The nodal approximations of elastic displacement vector \mathbf{U}^{j+1} and its velocity $\dot{\mathbf{U}}^{j+1}$ are defined by Newmark scheme [1, 5] as:

$$\begin{aligned}\mathbf{U}^{j+1} &= \mathbf{U}^j + \Delta t \dot{\mathbf{U}}^j + \frac{\Delta t^2}{2} \left[(1 - 2\beta) \ddot{\mathbf{U}}^j + 2\beta \ddot{\mathbf{U}}^{j+1} \right] \\ \dot{\mathbf{U}}^{j+1} &= \dot{\mathbf{U}}^j + \Delta t \left[(1 - \gamma) \ddot{\mathbf{U}}^j + \gamma \ddot{\mathbf{U}}^{j+1} \right],\end{aligned}\quad (24)$$

where $\ddot{\mathbf{U}}^j$ is an approximation of the mechanical acceleration at node t_j and γ, β are parameters of the scheme. However, the nodal approximations of temperature increment Θ^{j+1} and heat flux \mathbf{Q}^{j+1} are determined by the generalized trapezoidal rule [1, 5] with parameter γ :

$$\Theta^{j+1} = \Theta^j + \Delta t \left[(1 - \gamma) \dot{\Theta}^j + \gamma \dot{\Theta}^{j+1} \right], \quad (25)$$

$$\mathbf{Q}^{j+1} = \mathbf{Q}^j + \Delta t \left[(1 - \gamma) \dot{\mathbf{Q}}^j + \gamma \dot{\mathbf{Q}}^{j+1} \right], \quad (26)$$

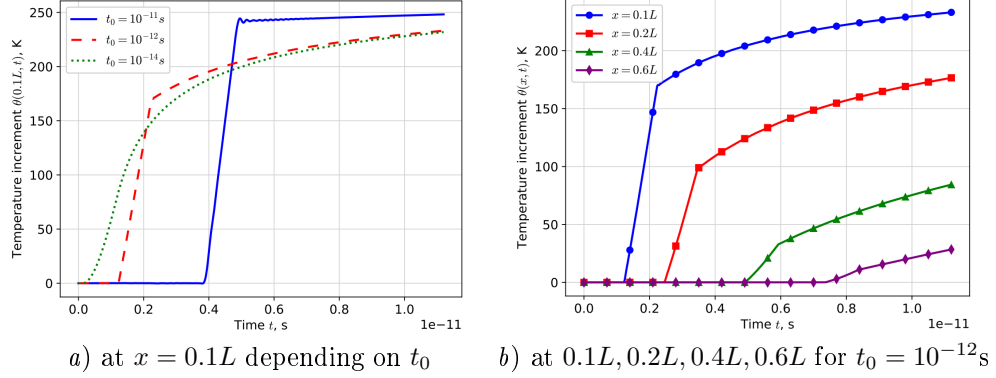
where $\dot{\Theta}^j$ is an approximation of the velocity of temperature increment and $\dot{\mathbf{Q}}^j$ is an approximation of the velocity of heat flux at node t_j .

Then we obtain the following numerical scheme:

$$\left\{ \begin{array}{l} \text{given } \Delta t > 0, t_0 > 0, 0 \leq \gamma \leq 1, 0 \leq \beta \leq \frac{1}{2}, \\ (\ddot{\mathbf{U}}^j, \dot{\mathbf{U}}^j, \mathbf{U}^j, \dot{\Theta}^j, \Theta^j, \dot{\mathbf{Q}}^j, \mathbf{Q}^j); \\ \text{find } (\ddot{\mathbf{U}}^{j+1}, \dot{\Theta}^{j+1}, \dot{\mathbf{Q}}^{j+1}) \text{ such that} \\ \left(\begin{array}{ccc} \mathbf{M} + \Delta t \gamma \mathbf{A} + \Delta t^2 \beta \mathbf{C} & -\Delta t \gamma \mathbf{B}^T & 0 \\ \Delta t \gamma \mathbf{B} & \mathbf{S} & \Delta t \gamma \mathbf{W}^T \\ 0 & -\Delta t \gamma \mathbf{W} & t_0 \mathbf{K} + \Delta t \gamma \mathbf{K} \end{array} \right) \times \left(\begin{array}{c} \ddot{\mathbf{U}}^{j+1} \\ \dot{\Theta}^{j+1} \\ \dot{\mathbf{Q}}^{j+1} \end{array} \right) = \\ = \left(\begin{array}{c} \mathbf{L}_{j+1} - \mathbf{A} \tilde{\mathbf{U}}^{j+1} - \mathbf{C} \tilde{\mathbf{U}}^{j+1} + \mathbf{B}^T \tilde{\Theta}^{j+1} \\ \mathbf{F}_{j+1} - \mathbf{B} \tilde{\mathbf{U}}^{j+1} - \mathbf{W}^T \tilde{\mathbf{Q}}^{j+1} \\ \mathbf{W} \tilde{\Theta}^{j+1} - \mathbf{K} \tilde{\mathbf{Q}}^{j+1} \end{array} \right), \end{array} \right. \quad (27)$$

where we use predictors

$$\begin{aligned}\tilde{\mathbf{U}}^{j+1} &= \mathbf{U}^j + \Delta t \dot{\mathbf{U}}^j + \frac{\Delta t^2}{2} (1 - 2\beta) \ddot{\mathbf{U}}^j, \\ \tilde{\mathbf{U}}^{j+1} &= \dot{\mathbf{U}}^j + \Delta t (1 - \gamma) \ddot{\mathbf{U}}^j, \\ \tilde{\Theta}^{j+1} &= \Theta^j + \Delta t (1 - \gamma) \dot{\Theta}^j, \\ \tilde{\mathbf{Q}}^{j+1} &= \mathbf{Q}^j + \Delta t (1 - \gamma) \dot{\mathbf{Q}}^j.\end{aligned}\quad (28)$$

Fig. 1. Temperature increment θ

Afterwards, using the following correctors, we compute the unknown values at time step $j + 1$:

$$\begin{aligned}\mathbf{U}^{j+1} &= \tilde{\mathbf{U}}^{j+1} + \Delta t^2 \beta \ddot{\mathbf{U}}^{j+1}, \\ \dot{\mathbf{U}}^{j+1} &= \tilde{\dot{\mathbf{U}}}^{j+1} + \Delta t \gamma \ddot{\mathbf{U}}^{j+1}, \\ \boldsymbol{\Theta}^{j+1} &= \tilde{\boldsymbol{\Theta}}^{j+1} + \Delta t \gamma \dot{\boldsymbol{\Theta}}^{j+1}, \\ \mathbf{Q}^{j+1} &= \tilde{\mathbf{Q}}^{j+1} + \Delta t \gamma \dot{\mathbf{Q}}^{j+1}.\end{aligned}\tag{29}$$

The values for $\ddot{\mathbf{U}}^0$, $\dot{\boldsymbol{\Theta}}^0$, $\dot{\mathbf{Q}}^0$ that are needed as an input for the first step of the aforementioned time integration scheme are easily obtained by solving a system of linear algebraic equations that corresponds to Cauchy problem (21) for $t = 0$.

The numerical scheme defined by (27)-(29) is a partial case of the scheme presented in [14] and therefore it is also unconditionally stable if its parameters are $\gamma = \frac{1}{2}$ and $\beta = \frac{1}{4}$.

6. RESULTS AND DISCUSSION

We replicate the numerical experiment done in [14] assuming that the material does not exhibit piezoelectric and pyroelectric properties. A solid bar of length $L = 10^{-8}$ m is considered. The behavior of the waves in the bar is examined during a very short time interval $T = 11.2 \cdot 10^{-12}$ s.

The left edge of the bar is subject to the ramp-type heating:

$$\theta(0, t) = \theta_c \begin{cases} \frac{t}{t_p}, & 0 \leq t \leq t_p \\ 1, & t_p \leq t \leq T \end{cases}, \tag{30}$$

where $t_p = 10^{-12}$ s and $\theta_c = 293$ K. At the same time the right edge of the bar is kept at the initial temperature:

$$\theta(L, t) = 0, \quad 0 \leq t \leq T. \tag{31}$$

The boundary conditions for mechanical field are of Neumann type:

$$\sigma = \bar{\sigma} = 0 \text{ N/m}^2 \text{ on } \Gamma_\sigma \times [0, T], \quad \Gamma_\sigma = \{x = 0\} \cup \{x = L\}. \tag{32}$$

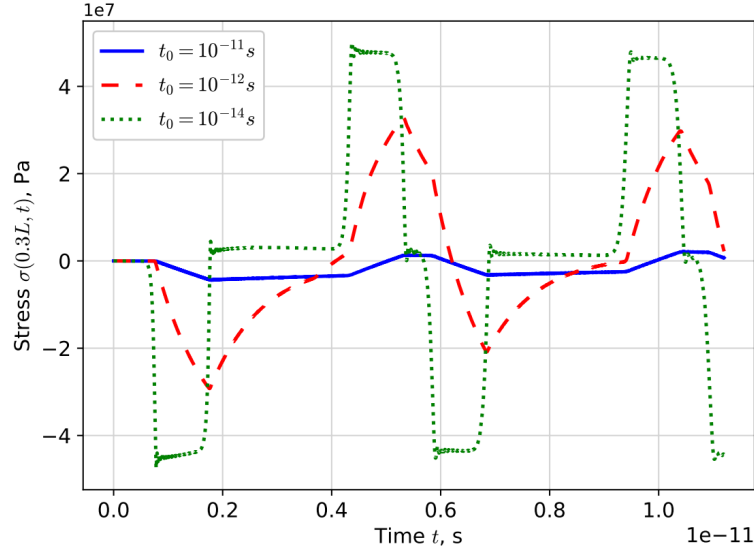


Fig. 2. Stress σ at $x = 0.3L$ depending on t_0

The initial conditions are taken to be zeros:

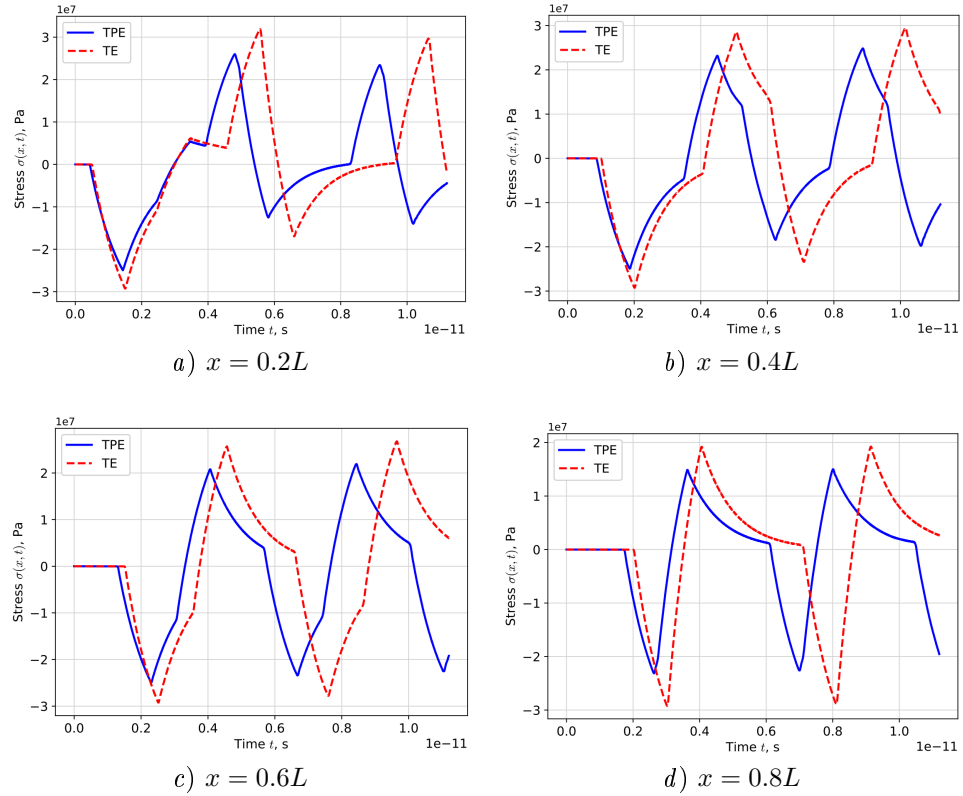
$$\begin{aligned} u(x, 0) &= 0, \\ u'(x, 0) &= 0, \\ \theta(x, 0) &= 0, \\ q(x, 0) &= 0, \quad \forall x \in [0, L]. \end{aligned} \tag{33}$$

To be able to compare the obtained numerical solution with the results described in [14] and [15] we take the same values of physical coefficients of a solid as in those papers (PZT-4 ceramics is considered, but the coefficients that correspond to piezoeffect and pyroeffect are neglected). Besides, we choose the same discretization parameters as in work [14]: $N = 1024$ finite elements with piecewise linear approximations, the time interval $[0, T]$ is divided into $N_T = 4096$ subintervals, and time integration scheme parameters are $\gamma = \frac{1}{2}$, $\beta = \frac{1}{4}$.

Fig. 1a shows temperature increment θ variation over time for position $x = 0.1L$ for the relaxation time parameter t_0 values equal to $10^{-11}s$, $10^{-12}s$ and $10^{-14}s$ respectively. The influence of this parameter is clearly seen and the results are almost identical to the ones some of the authors of the current paper obtained in [14] for Lord-Shulman thermopiezoelectricity problem. Fig. 1b shows temperature increment θ at $x = 0.1L, 0.2L, 0.4L, 0.6L$ for $t_0 = 10^{-12}s$ and also is almost identical to the one demonstrated in [14].

We can measure the difference between thermoelasticity solution $\theta(x, t)$ depicted on Fig. 1b and thermopiezoelectricity one $\theta_{piezo}(x, t)$ described in [14] using the norm in space $L^2([0, T])$. The coefficient of relative difference can be defined in percents by the following expression:

$$d = \frac{||\theta(x, t)||_{L^2([0, T])} - ||\theta_{piezo}(x, t)||_{L^2([0, T])}}{||\theta_{piezo}(x, t)||_{L^2([0, T])}} \cdot 100\%. \tag{34}$$

Fig. 3. Stress σ at different positions of the bar for $t_0 = 10^{-12}$ s

The calculated norms and relative differences are shown in Table 1.

Table 1

$L^2([0, T])$ norm difference of temperature increment solutions

x	$\ \theta(x, t)\ _{L^2([0, T])}$	$\ \theta_{piezo}(x, t)\ _{L^2([0, T])}$	$d, \%$
$0.1L$	$6.43696469 \cdot 10^{-4}$	$6.43819452 \cdot 10^{-4}$	0.019
$0.2L$	$4.17475046 \cdot 10^{-4}$	$4.17660451 \cdot 10^{-4}$	0.044
$0.4L$	$1.46564265 \cdot 10^{-4}$	$1.46750905 \cdot 10^{-4}$	0.127
$0.6L$	$3.49079686 \cdot 10^{-5}$	$3.50368990 \cdot 10^{-5}$	0.368

In general, we can state, that in case of ramp-type heating of the bar, the speed of the thermal wave does not differ significantly for thermoelasticity and thermopiezoelectricity cases.

However, for stress $\sigma(x, t)$ there is a significant difference between current thermoelasticity (TE) solution and the thermopiezoelectricity (TPE) one described in [14]. Fig. 2 shows the influence of the relaxation time parameter t_0 on the obtained stress solution $\sigma(x, t)$. Although at the first sight it resembles the one from [14], the difference is in stress wave amplitudes (they are larger for TE solution) and the stress wave propagates

with smaller speed for all values of t_0 than in TPE solution demonstrated in [14]. The aforementioned differences highlight the impact of piezoeffect and pyroeffect phenomena on stress waves in solids.

Fig. 3 describes more detailly the difference between TE and TPE solutions $\sigma(x, t)$ at several points $x = 0.2L, 0.4L, 0.6L, 0.8L$ for $t_0 = 10^{-12}$ s. The same comparison was done by other researchers in [15] and our results coincide with theirs both qualitatively and quantitatively.

7. CONCLUSIONS

Lord-Shulman thermoelasticity model is considered. The initial boundary value problem is formulated similarly to how the corresponding thermopiezoelectricity one is defined in some of the authors' previous works [12–14].

The problem is solved using the adopted technique from the work [14]: transforming it into the variational problem and using finite element method complemented by a hybrid time integration procedure based on Newmark scheme and generalized trapezoidal rule. The obtained numerical scheme is also unconditionally stable for $\gamma = \frac{1}{2}$, $\beta = \frac{1}{4}$ as a partial case of the one described in [14].

The approximate solutions were obtained using a Python implementation of the proposed numerical scheme. While for temperature increment $\theta(x, t)$ the results are almost identical to the ones of the thermopiezoelectricity problem described in [14], for stress $\sigma(x, t)$ the solutions differ a lot. Besides, this difference in stress $\sigma(x, t)$ solutions demonstrated by us are completely in accordance with the results depicted by other researchers in [15].

REFERENCES

1. Bathe K.J. Finite Element Procedures. 2nd ed. / K.J. Bathe. – Watertown: K.J. Bathe, 2014. – 1043 p.
2. Eshkofti K. A gradient-enhanced physics-informed neural network (gPINN) scheme for the coupled non-fickian/non-fourierian diffusion-thermoelasticity analysis: A novel gPINN structure / K. Eshkofti, S.M. Hosseini // Engineering Applications of Artificial Intelligence. – 2023. – Vol. 126. – P. 106908.
3. Eslami M.R. Theory of Elasticity and Thermal Stresses: Explanations. – Problems and Solutions. – ol. 197. in Solid Mechanics and Its Applications / M.R. Eslami, R.B. Hetnarki, J. Ignaczak, N. Noda, N. Sumi, Y. Tanigawa. – Dordrecht: Springer Netherlands, 2013. – 789 p.
4. Hetnarski R.B. Thermal Stresses-Advanced Theory and Applications, vol. 158. in Solid Mechanics and Its Applications. 2nd ed. / R.B. Hetnarki, M.R. Eslami. – Cham: Springer International Publishing, 2019. – 636 p.
5. Hughes T.J.R. The Finite Element Method. Linear Static and Dynamic Finite Element Analysis / T.J.R. Hughes // Dover Publications, 2000. – 704 p.
6. Jani S.M.H. Generalized thermo-electro-elasticity of a piezoelectric disk using Lord-Shulman theory / S.M.H. Jani, Y. Kiani // Journal of Thermal Stresses. – 2020. – Vol. 43. – P. 473–488.
7. Jani S.M.H. Generalized piezothermoelasticity of hollow spheres under thermal shock using Lord-Shulman theory / S.M.H. Jani, Y. Kiani, Y. Tadi Beni // Journal of Thermal Stresses. – 2024. – Vol. 47. – P. 347–362.
8. Kapuria S. Thermo-electroelastic shock waves in piezoelectric media: An enriched finite element solution based on generalized piezothermoelasticity / S. Kapuria, A. Kumar // Mechanics of Advanced Materials and Structures. – 2021. – Vol. 48. – P. 2267–2279.

9. Kiani Y. Nonlinear generalized thermoelasticity of an isotropic layer based on Lord-Shulman theory / Y. Kiani, M.R. Eslami // *European Journal of Mechanics. – A/Solids.* – 2017. – Vol. 61. – P. 245–253.
10. Kumar A. Wave packet enriched finite element for generalized thermoelasticity theories for thermal shock wave problems / A. Kumar, S. Kapuria // *Journal of Thermal Stresses.* – 2018. – Vol. 41. – P. 1080–1099.
11. Lord H.W. A generalized dynamical theory of thermoelasticity / H.W. Lord, Y. Shulman // *Journal of the Mechanics and Physics of Solids.* – 1967. – Vol. 15. – P. 299–309.
12. Stelmashchuk V. Numerical solution of Lord-Shulman thermopiezoelectricity dynamical problem / V. Stelmashchuk, H. Shynkarenko // *AIP Conf. Proc.* – 2018. – Vol. 1922. – 040006. – P. 1–10.
13. Stelmashchuk V.V. Well-posedness of the Lord-Shulman variational problem of thermopiezoelectricity / V.V. Stelmashchuk, H.A. Shynkarenko // *Journal of Mathematical Sciences.* – 2019. – Vol. 238. – P. 139–153.
14. Stelmashchuk V. Stability of hybrid time integration scheme for Lord-Shulman thermopiezoelectricity / V. Stelmashchuk, H. Shynkarenko // *Results in Applied Mathematics.* – 2024. – Vol. 23. – P. 100467.
15. Sumi N. Solution for thermal and mechanical waves in a piezoelectric plate by the method of characteristics / N. Sumi, F. Ashida // *J. Thermal Stresses.* – 2003. – Vol. 26. – P. 1113–1123.
16. Wang Y.-Z. A unified generalized thermoelasticity solution for the transient thermal shock problem / Y.-Z. Wang, X.-B. Zhang, X.-N. Song, // *Acta Mech.* – 2012. – Vol. 223. – P. 735–743.
17. Zhao J. Thermoelastic wave propagation damping in a hollow FG-GPLRC cylinder with the spinning motion / J. Zhao, P. Liang, R. Yang, Y. Zhang, M.A. Khadimallah, A. Ebtekar // *Thin-Walled Structures.* – 2022. – Vol. 177. – P. 109367.

*Article: received 04.10.2024**revised 24.10.2024**printing adoption 14.11.2024*

СКІНЧЕННОЕЛЕМЕНТНИЙ АНАЛІЗ ДИНАМІЧНОЇ ЗАДАЧІ ТЕРМОПРУЖНОСТІ ЛОРДА-ШУЛЬМАНА

В. Стельмашук, Р. Петришин, Г. Шинкаренко

Львівський національний університет імені Івана Франка,

вул. Університетська 1, Львів, 79000, Україна

e-mail: vitalii.stelmashchuk@lnu.edu.ua,

roman.petryshyn.apmi@lnu.edu.ua, heorhiy.shynkarenko@lnu.edu.ua

Розглянуто початково-крайову задачу термопружності Лорда-Шульмана. Потім вона перетворюється у відповідну їй варіаційну задачу. Використовуючи напівдискретизацію Гальоркіна за просторовими змінними з базисними функціями методу скінчених елементів, варіаційна задача зводиться до матричної задачі Коші. Для дискретизації в часі отриманої задачі Коші ми адаптуємо гібридну схему інтегрування в часі (що базується на схемі Ньюмарка й узагальненому методі трапецій), яка початково була розроблена для задачі термоп'єзоелектрики Лорда-Шульмана. У чисельних експериментах розглядається нагрівання одного з кінців стрижня з лінійною зміною температури. Далі розв'язки, отримані запропонованою чисельною схемою, порівнюють з розв'язками відповідної задачі термоп'єзоелектрики Лорда-Шульмана, наявними в літературі. Зокрема, підтверджено, що на поведінку хвилі

напружень у стрижні помітно впливає п'єзо- та піроефект. Крім того, отримані чисельні результати відповідають результатам, які отримали інші дослідники за допомогою інших методів.

Ключові слова: термопружність Лорда-Шульмана, початково-крайова задача, варіаційна задача, метод скінченних елементів, схема Ньюмарка, узагальнений метод трапецій.